Aza- and Oxadithiolates are Proton Relays in Functional Models for the [FeFe]-Hydrogenases

Bryan E. Barton, Matthew T. Olsen, and Thomas B. Rauchfuss*
School of Chemical Sciences, University of Illinois, Urbana, IL 61801

Supporting Information

1) Experimental Procedures

2) Supporting Figures

3) Supporting Information References

1.) Experimental Procedures

Manipulations were conducted using standard Schlenk techniques. Solvents were filtered through activated alumina and subsequently degassed. ^{1}H and ^{31}P NMR spectra were acquired on a Unity Varian 500 or a Unity Varian 600 spectrometer. IR spectra were collected on a Mattson Infinity Gold FTIR spectrometer. *Cis*-1,2-bis(diphenylphosphino)ethylene (dppv) and $HBF_4{\cdot}Et_2O$ solution were purchased from Aldrich. $Fe_2(S_2C_3H_6)(CO)_2(dppv)_2$ (**1**),[1] $Fe_2[S_2(CH_2)_2NH](CO)_2(dppv)_2$ (**2**),[1] $Fe_2(S_2C_2H_4O)(CO)_6$ (**3**),[2] and $[H(Et_2O)_2]BAr^F{}_4$[3] were prepared according to literature procedures ($BAr^F{}_4^-$ = $B(C_6H_3\text{-}3,5\text{-}(CF_3)_2)_4^-$).

$Fe_2[(SCH_2)_2O](CO)_4(dppv)$. To a solution of 0.518 g (1.34 mmol) $Fe_2(S_2C_2H_4O)(CO)_6$ and 0.549 g (1.38 mmol) of dppv in 20 mL of MeCN was added 0.100 g (0.133 mmol) of Me_3NO in 5 mL of MeCN. The solution immediately darkened and over several hours thickened with a brown precipitate. Solvent was removed in vacuo, the solid was dissolved in 5 mL of CH_2Cl_2, and precipitated by addition of 40 mL of hexane. This process was repeated twice to give a fluffy golden powder of the crude compound that was sufficiently pure for the next step. Yield: 0.878 g (90%). ^{1}H NMR (200 MHz, CD_2Cl_2, 20 °C): δ ~8.0 (m, 4H, C_2H_2), ~7.5 – 7.2 (m, 20H, C_2H_2P), 3.86 (d, SCH_2, $J_{H,H}$ = 9.6 Hz), 3.37 (d, SCH_2, $J_{H,H}$ = 8.4 Hz). ^{31}P NMR (200 MHz, CD_2Cl_2, 20 ºC): δ 96.9 (s, dppv), 83.6 (s, dppv). FT-IR (CH_2Cl_2): ν_{CO} = 2026, 1955, 1918 cm^{-1}. FD-MS: m/z = 728.0 ($[Fe_2[(SCH_2)_2O](CO)_4(dppv)]^+$).

$Fe_2[(SCH_2)_2O](CO)_2(dppv)_2$, (3). A solution of 0.266 g of $Fe_2[(SCH_2)_2O](CO)_4(dppv)$ (0.37 mmol) and 0.160 g of dppv (0.40 mmol) in 75 mL of toluene was photolyzed with a 100 W UV immersion lamp, λ_{max} = 356 nm (Spectroline), until the IR spectrum showed complete consumption of the starting material (~20 hours). The solution was dried in vacuo, redissolved in 5 mL of CH_2Cl_2 and precipitated upon addition of 40 mL of hexanes. This process was repeated twice or until the filtrate was clear, yielding a dark green powder. Yield: 0.201g (51.5%). ^{1}H NMR (500 MHz, CD_2Cl_2, 20 ºC): δ 8.02 (m, 4H, C_2H_2P), 7.9 – 7.1 (m, 40H, C_2H_2P), 2.86 (2, $(SCH_2)_2O$, 4H). $^{31}P\{^{1}H\}$ NMR (202 MHz, CD_2Cl_2, 20 ºC): δ 91.6 (s). IR (CH_2Cl_2): ν_{CO} = 1891, 1871 cm^{-1}. Anal. Calcd for $C_{56}H_{48}Fe_2O_3P_4S_2$ (found): C, 62.94 (63.00); H, 4.53 (4.43).

$[HFe_2[(SCH_2)_2O](\mu\text{-}CO)(dppv)_2]BAr^F{}_4$, $[3H]BAr^F{}_4$. In a J. Young NMR tube CD_2Cl_2 was distilled onto $Fe_2[(SCH_2)_2O](CO)_2(dppv)_2$ (7 mg , 0.007 mmol) and $[H(Et_2O)_2][BAr^F{}_4]$ (7 mg, 0.007 mmol). The J. Young tube was then placed directly into a -78 °C bath and analyzed with low temperature NMR spectroscopy. High field ^{1}H NMR (600 MHz, CD_2Cl_2, -40 °C): δ - 2.7 (t, Fe-H, $^{2}J_{PH}$ = 72 Hz). $^{31}P\{^{1}H\}$ NMR (242 MHz, CD_2Cl_2, -40 °C): δ 99 (s), 94 (s), 89 (s), 69 (s). After isomerization: ^{1}H NMR (600 MHz, CD_2Cl_2, 25 °C): δ - 14.5 (qd, Fe-H, $J_{PH1,2,3}$ ~ 20 Hz, J_{PH4} ~ 7 Hz), δ - 15.4 (tt, Fe-H, $J_{PH1,2}$ ~ 20 Hz, $J_{PH3,4}$ ~ 7 Hz). $^{31}P\{^{1}H\}$ NMR (242 MHz, CD_2Cl_2, 25 °C): δ 89, 88; 86, 84, 83, 78.

Isomerization of [3(*t*-H)]$^+$ to [3(μ-H)]$^+$. In a J. Young NMR tube CD_2Cl_2 (0.7 mL) was distilled onto **3** (7 mg, 0.007 mmol), $[H(Et_2O)_2]BAr^F{}_4$ (7 mg, 0.007 mmol), and hexamethylbenzene (0.5 mg, 0.005 mmol). The J. Young tube was then placed into a -40 °C bath and analyzed with low temperature NMR spectroscopy. Data were collected as an array over 2 h showing nearly complete consumption of **2**H$^+$ and growth of two isomers of **2**μ$^+$. The terminal hydride triplet at δ -2.7 was integrated from each FID against the internal standard hexamethylbenzene. The isomerization of terminal hydride followed first order kinetics (see figure S15).

Preparation of [HPPh$_3$]BAr$^F{}_4$. A solution of $[H(Et_2O)_2][BAr^F{}_4]$ (0.385 g, 0.377 mmol) in Et_2O (10 mL) at -40 °C was transferred via cannula into a solution of PPh_3 (0.097 g, 0.370 mmol) in Et_2O (10 mL) at -40 °C. Solvent was removed under vacuum, leaving a white solid. Yield: 0.350 g (83%). $^{31}P\{^1H\}$ NMR (242 MHz, CD_2Cl_2, 20 °C): δ 7.0 (s). ^1H NMR (600 MHz, CD_2Cl_2, 20 °C): δ 8.28 (d, 1H, $[HPPh_3]^+$, J_{PH} = 498 Hz), 7.6-8.0 (m, 15H, [HP*Ph$_3$*]), 7.55 (s, 4H, *p*-C*H,* $[BAr^F{}_4]^-$), 7.73 (s, 8H, *o*-CH, $[BAr^F{}_4]^-$).

Electrochemistry. Cyclic voltammetry experiments were carried out in a ca. 20-mL one-compartment glass cell. The working electrode was a glassy carbon disk (0.3 cm in diameter). The reference electrode for experiments conducted less than 0 °C was a pseudo-reference silver wire, for experiments > 0 °C, a Ag/AgCl electrode (ca. -0.50 V vs Fc/Fc^+) was employed. The counter electrode was a Pt wire. The electrolyte was 0.1 M Bu_4NPF_6. The concentration of the organometallic complex was 1 mM.

Proton Reduction Catalysis Cyclic Voltammetry for [3(*t*-H)]BF$_4$. A at -40 °C solution of **3** (7.5 mg, 0.007 mmol) in 6 mL CH_2Cl_2 was treated with aliquots (10 μL, 0.07 mmol) of a 0.691 M $HBF_4{\cdot}Et_2O$ solution in CH_2Cl_2. Cyclic voltammograms were collected at 50 mV/s.

Proton Reduction Catalysis Cyclic Voltammetry for [2(*t*-H)]BF$_4$. A -40 °C solution of **2** (7.5 mg, 0.007 mmol) in 6 mL CH_2Cl_2 was treated at -40 °C with aliquots (100 μL, 0.07 mmol) of a solution of 0.0691 M $[HPMe_2Ph]BF_4$ in CH_2Cl_2. Cyclic voltammograms were recorded at 50 mV/s.

2) Supplemental Figures

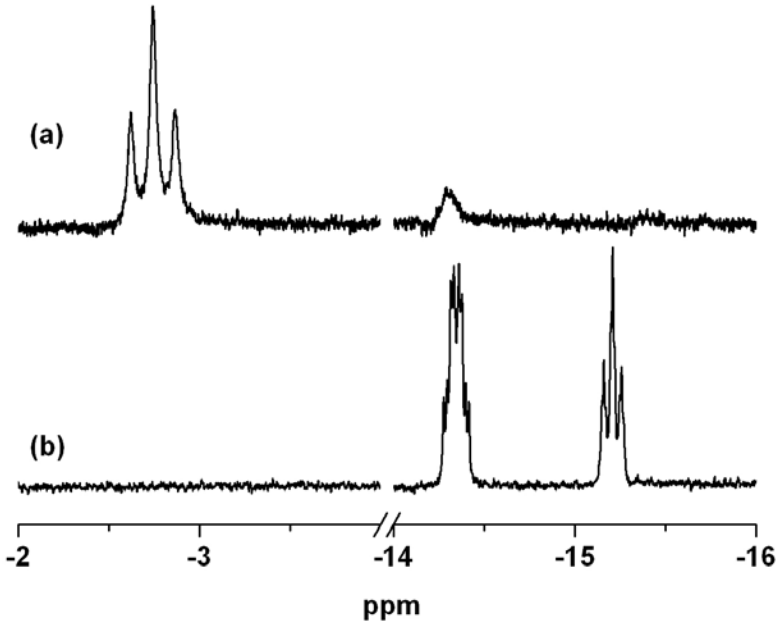

Figure S1. ^{1}H NMR spectra of a CD_2Cl_2 solution of **3** after protonation with $[H(Et_2O)_2]BAr^F{}_4$.

a: The kinetically-favored terminal hydride (-75 °C, 600 MHz) showing [**3**(*t*-H)]$BAr^F{}_4$ as well as a small amount of the first isomer of the bridging hydride (δ -14.4)

b: After isomerizing to [**3**(μ-H)]$BAr^F{}_4$ upon warming to 25 °C (recorded at 500 MHz). The bridging hydride exists as two predominant isomers at δ - 14.5 (qd, Fe-H, $J_{PH1,2,3}$ ~ 20 Hz, J_{PH4} ~ 7 Hz for the asymmetric (apical,basal-dppv)(basal,basal-dppv) isomer) and at δ - 15.4 (tt, Fe-H, $J_{PH1,2}$ ~ 20 Hz, $J_{PH3,4}$ ~ 7 Hz for the dissymmetric (apical,basal-dppv)$_2$ isomer.

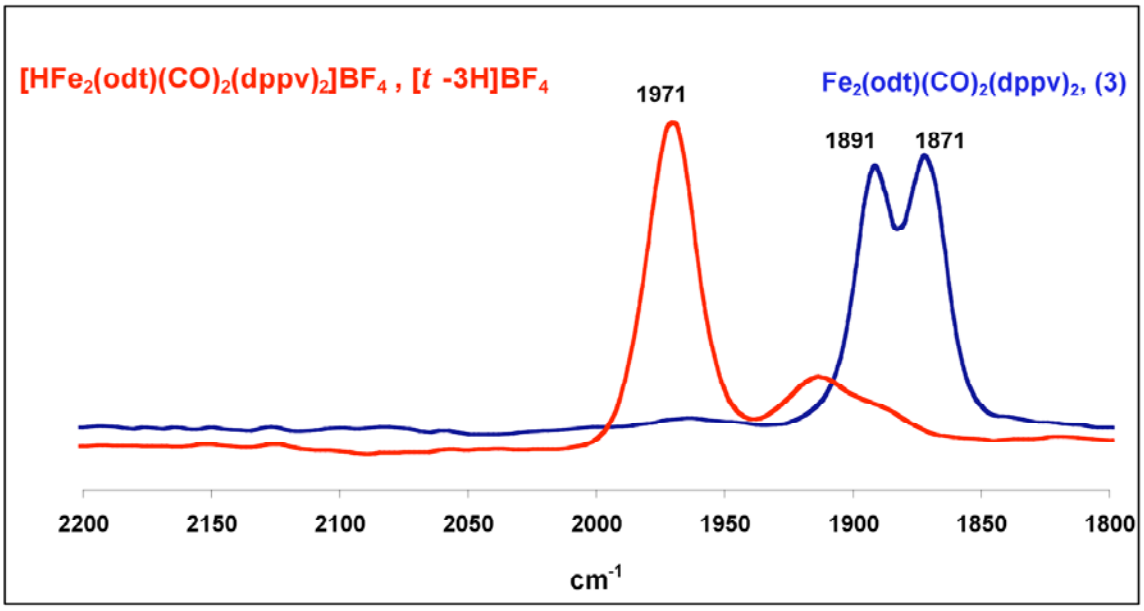

Figure S2. FT-IR spectra (-40 °C, CH_2Cl_2) of **3** (blue) and [**3**(*t*-H)]BF_4 (red).

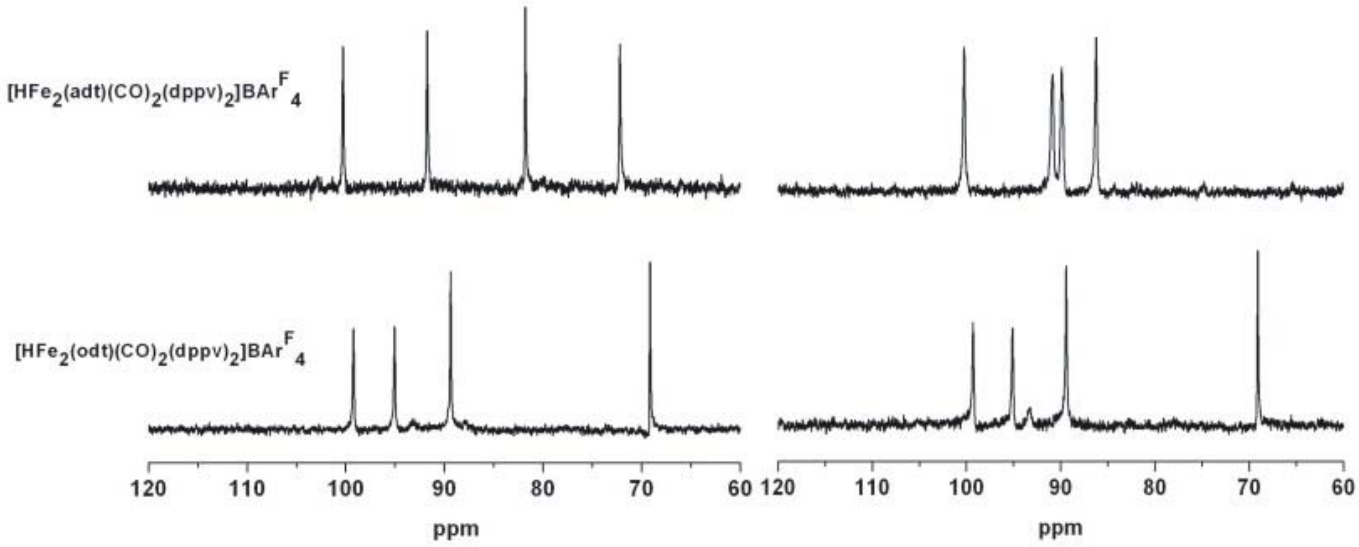

Figure S3. $^{31}P\{^{1}H\}$ NMR (242 MHz, CD_2Cl_2, -75 °C) spectra before (left) and after (right) treatment of solutions (CD_2Cl_2, -75 °C) of [**2**(*t*-H)]BAr^F_4 and [**3**(*t*-H)]BAr^F_4 with ~100 equiv of Et_3N. Upon addition of NEt_3 to [**2**(*t*-H)]BAr^F_4, resulting ^{31}P NMR (upper left) shows complete conversion to **2**, whereas for [**3**(*t*-H)]BAr^F_4, no change (lower left) is seen until warming near 0 °C (see Figure S4).

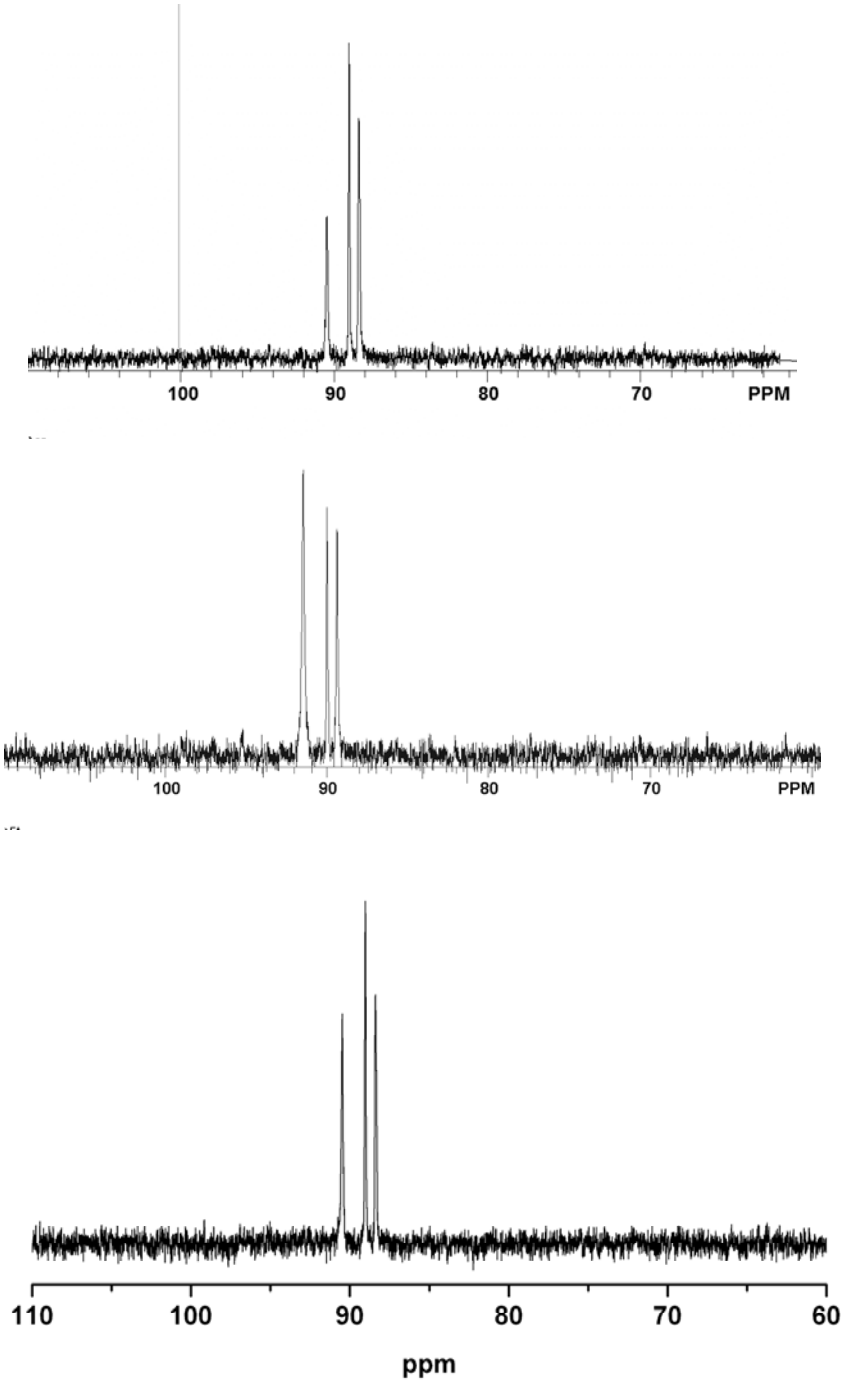

Figure S4. $^{31}P\{^{1}H\}$ NMR (242 MHz, CD_2Cl_2) spectra of solutions of [**3**(*t*-H)]BAr^F_4 treated with various bases (see below) at -97 °C, followed by warming to 20 °C, at which temperature the spectrum was recorded:
top: ~1 equiv of tetramethylguanidine,
middle: ~ 1 equiv of PPh_3,
bottom: >100 equiv NEt_3.
The spectra show about 50% conversion to **3** (δ 90) and about 50% conversion to [**3**(μ-H)]BAr^F_4 (single isomer, δ 89, 88), regardless of the strength and amount of base.

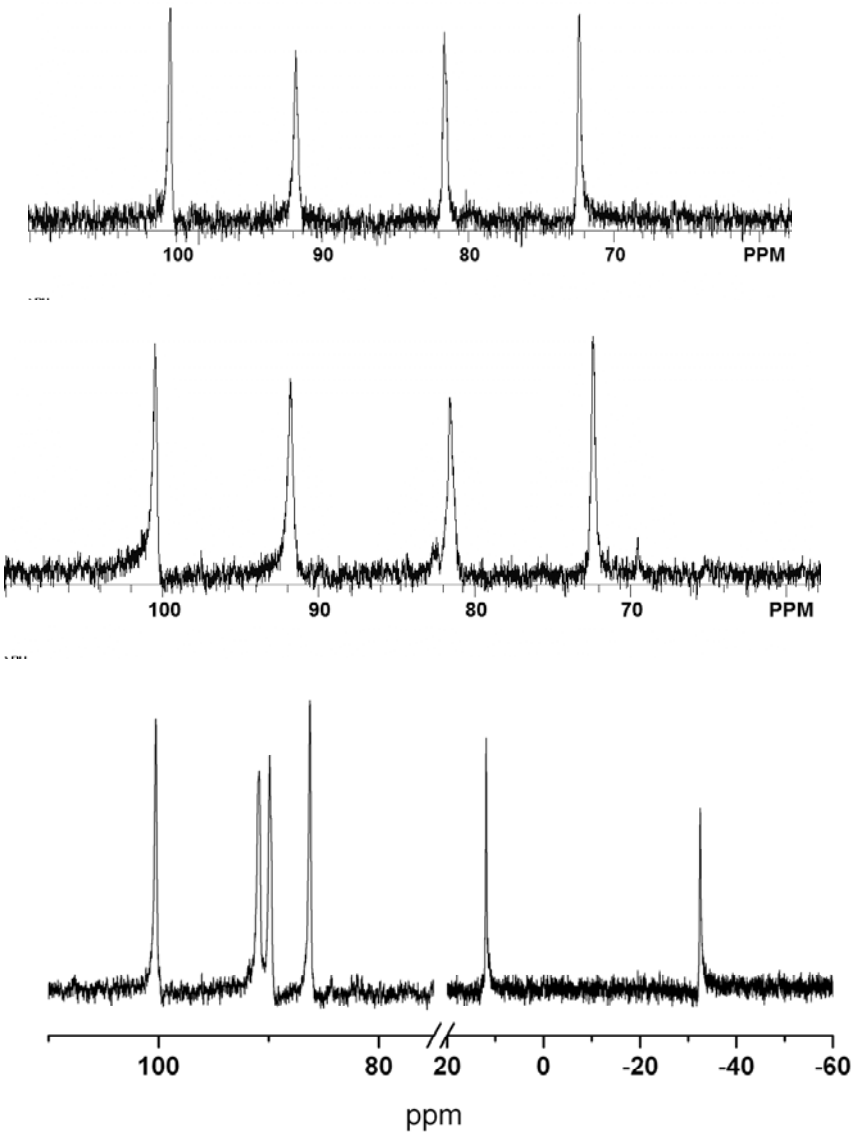

Figure S5. $^{31}P\{^{1}H\}$ NMR (242 MHz, CD_2Cl_2, -60 °C) spectra of [**2**(*t*-H)]BAr^F_4
top: before, and
middle: after treatment with ~1 equiv of PMe_2Ph (showing no reaction), then repeated by
bottom: treatment with ~ 1 equiv of PBu_3 showing complete conversion to **2** and some $[HPBu_3]BAr^F_4$ at δ 11 and PBu_3 at δ -33. Additions were conducted at -60 °C. In related experiments, CD_2Cl_2 (-80 °C) solutions of **1** and **3** were treated with $[H(OEt_2)_2]BAr^F_4$ (to give [**3**(*t*-H)]BAr^F_4 and [**1**(*t*-H)]BAr^F_4, respectively) followed by treatment with PPh_3, and then warming to room temperature. The sample of [**3**(*t*-H)]BAr^F_4 converted to a mixture of **3** and [**3**(μ-H)]BAr^F_4 (two isomers). The sample of [**3**(*t*-H)]BAr^F_4 converted to [**1**(μ-H)]BAr^F_4 (two isomers).

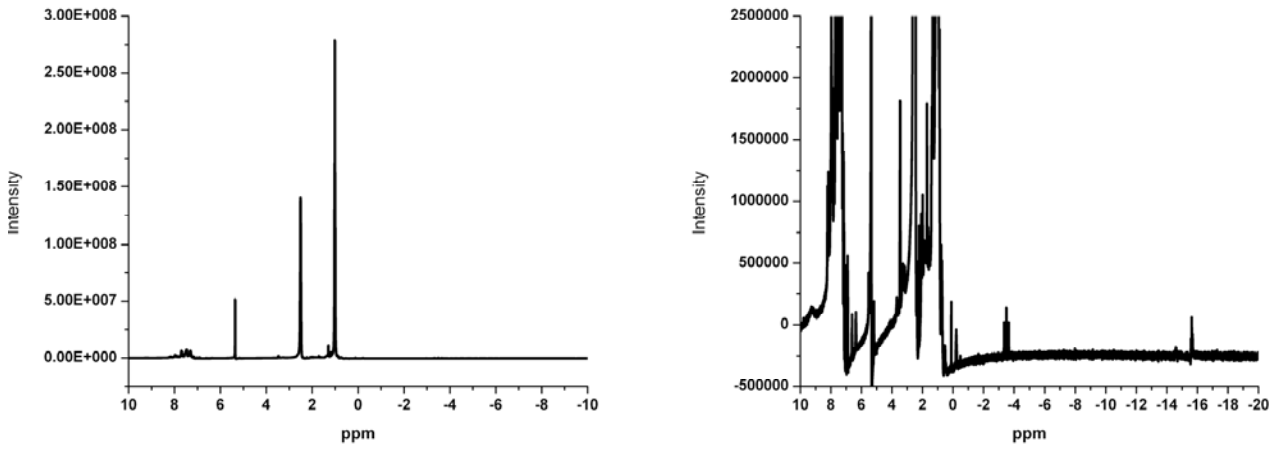

Figure S6. ^{1}H NMR (500 MHz, CD_2Cl_2) spectra (two views of the same spectrum) for solutions of [**1**(*t*-H)]BAr^F_4, generated at –35 °C, treated at that same temperature with a large excess of NEt_3 (δ 2.5, 1.0), followed by warming to 20 °C, whereupon the spectrum was recorded. The terminal hydride resonates at δ -3.5 (triplet) and the bridging hydride isomers at δ -14.5 and -15.7 (multiplets).

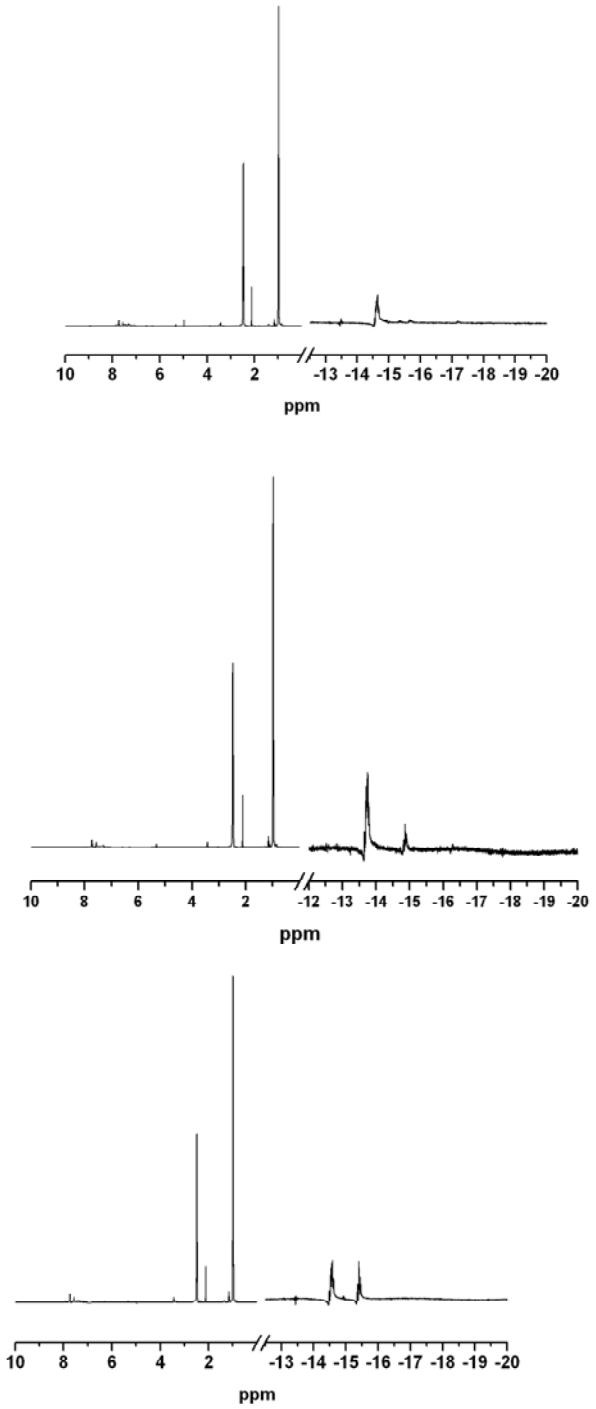

Figure S7. ^{1}H NMR (500 MHz, CD_2Cl_2) spectra of solutions of three μ-hydride compounds after treatment with large excess of NEt_3, after equilibration for 24 h at 20 °C. The high-field region (right) was magnified by 500x.
top spectrum: [**1**(μ-H)]BAr^F_4,
middle spectrum: [**2**(μ-H)]BAr^F_4,
bottom spectrum: [**3**(μ-H)]BAr^F_4.

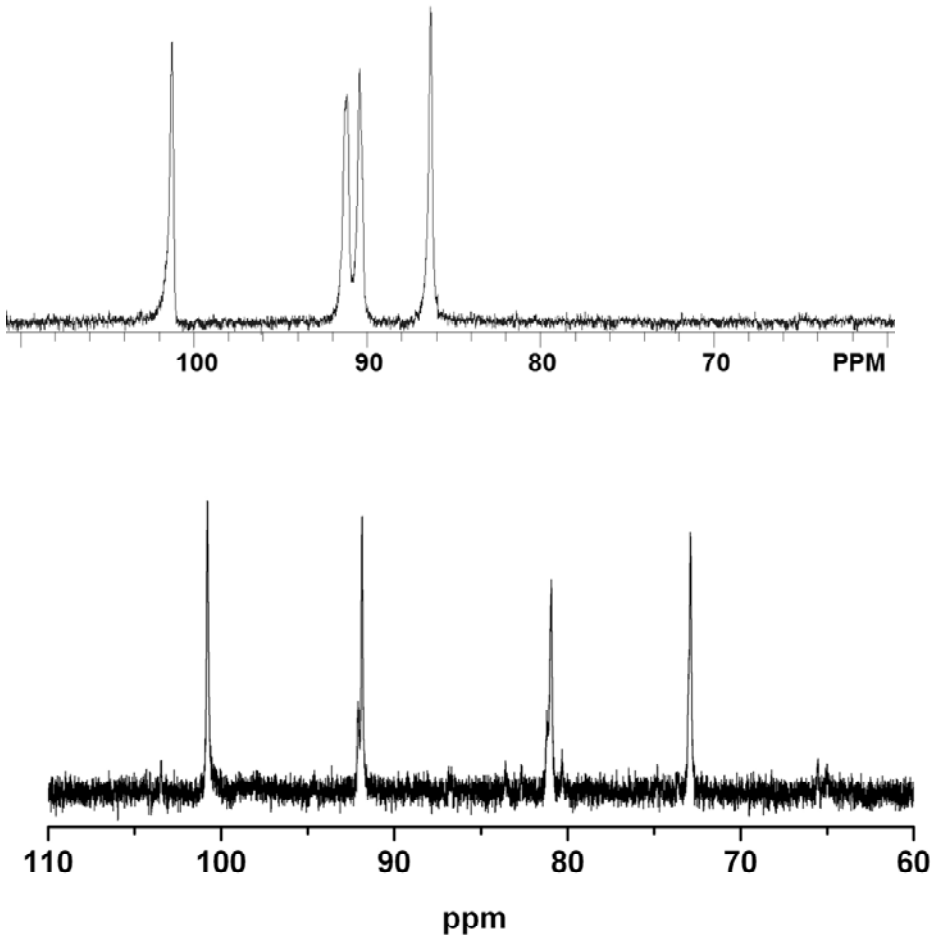

Figure S8. $^{31}P\{^{1}H\}$ NMR (242 MHz, CD_2Cl_2, -80 °C) spectra of solutions of **2** before (top spectrum) and after (bottom spectrum) treatment with ~1 equiv of $[HPPh_3]BAr^F{}_4$, showing complete conversion to [**2**(*t*-H)]$BAr^F{}_4$.

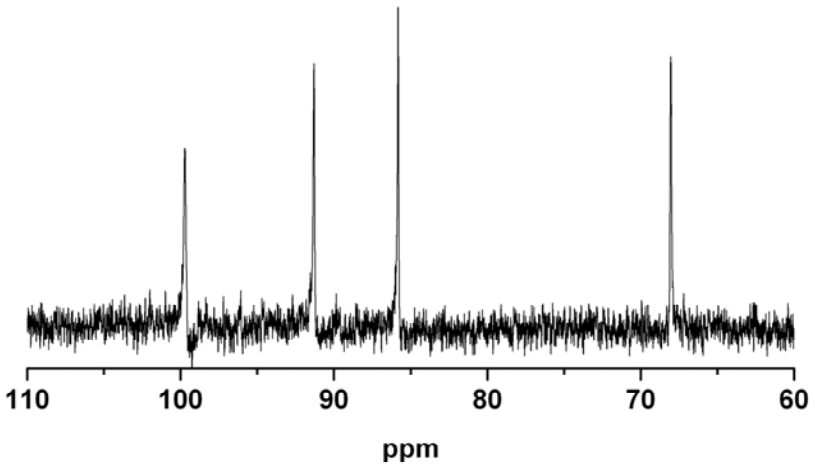

Figure S9. ^{31}P NMR (242 MHz, CD_2Cl_2) spectrum of [**1**(*t*-H)]BAr^F_4 generated by protonation of **1** with $[H(Et_2O)_2]BAr^F_4$ at -80 °C.

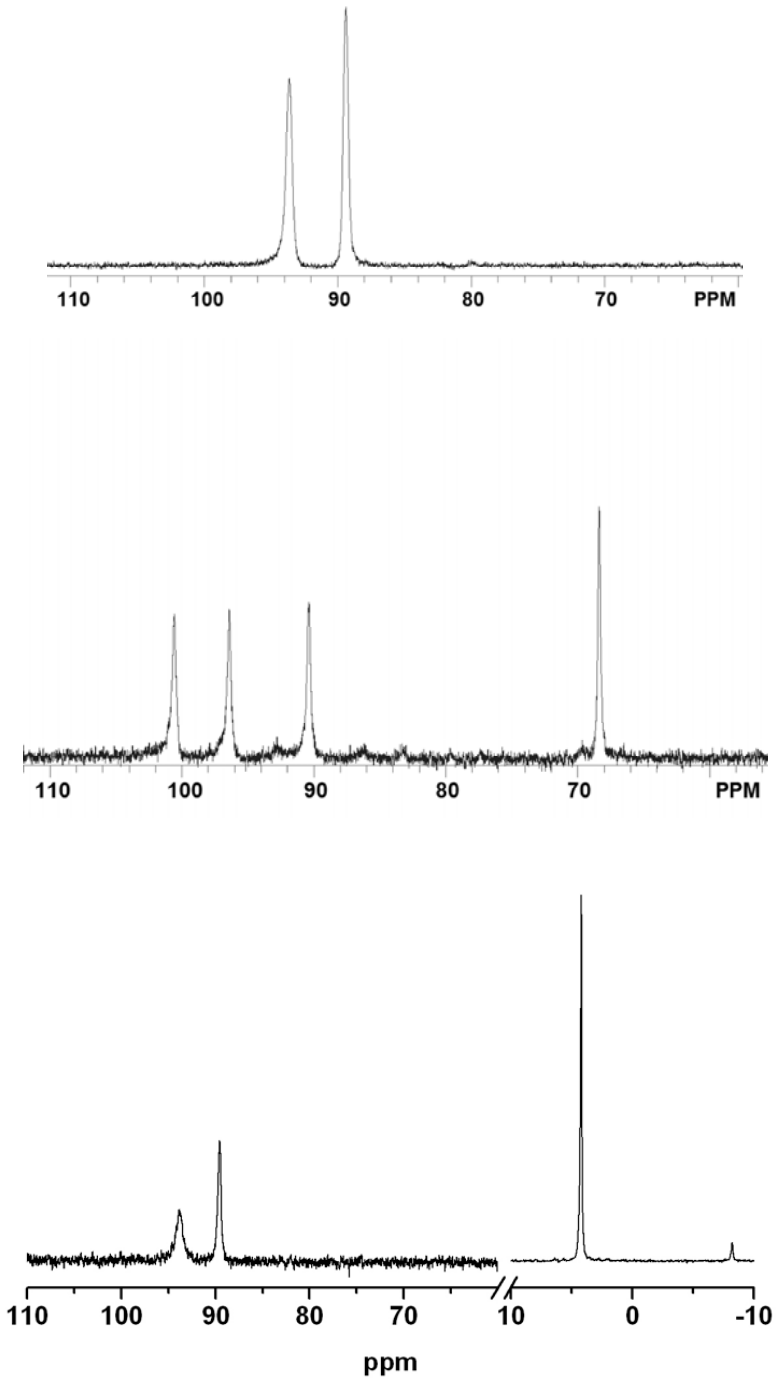

Figure S10. $^{31}P\{^{1}H\}$ NMR (242 MHz, CD_2Cl_2) spectra of **3** (-90 °C) before (top) and after (-90 °C, middle) treatment with 1 equiv of $[H(Et_2O)_2]BAr^F_4$, showing complete conversion to [**3**(*t*-H)]BAr^F_4. Bottom: Reaction of **3** (-80 °C, CD_2Cl_2) with ~1.2 equiv $[HPPh_3]BF_4$, showing mostly unreacted **3** (the right spectrum shows the signals for $HPPh_3^+$ as well as trace PPh_3. The low field signal is slightly broadened due to the onset of decoalescence.

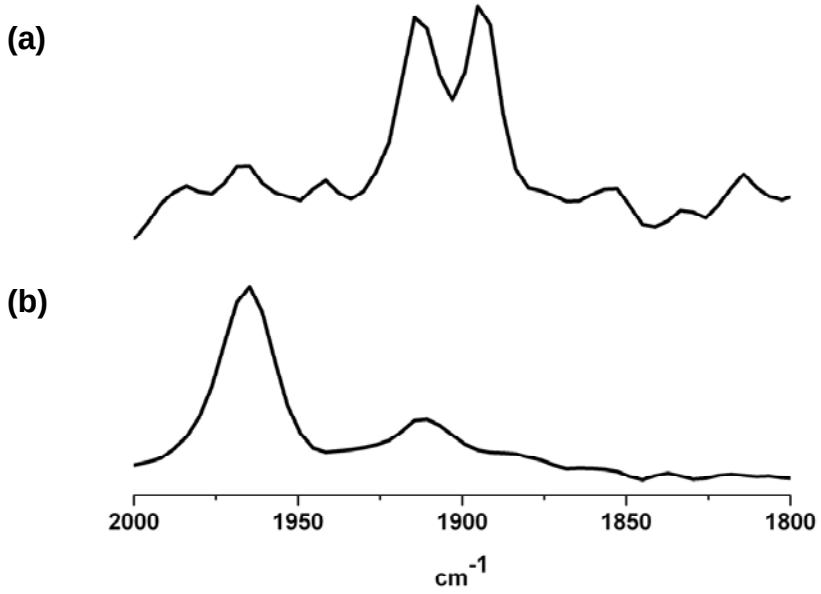

Figure S11. *In situ* ReactIR spectra of [**2**H]BAr$^{F}_{4}$ in MeOH (**a**, -40 °C, rough baseline arises in MeOH soln) showing *N*-protonated tautomer (1910, 1890 cm^{-1}) and in CH_2Cl_2 (**b**, -40 °C) showing terminal hydride tautomer (1965, 1910 cm^{-1}).

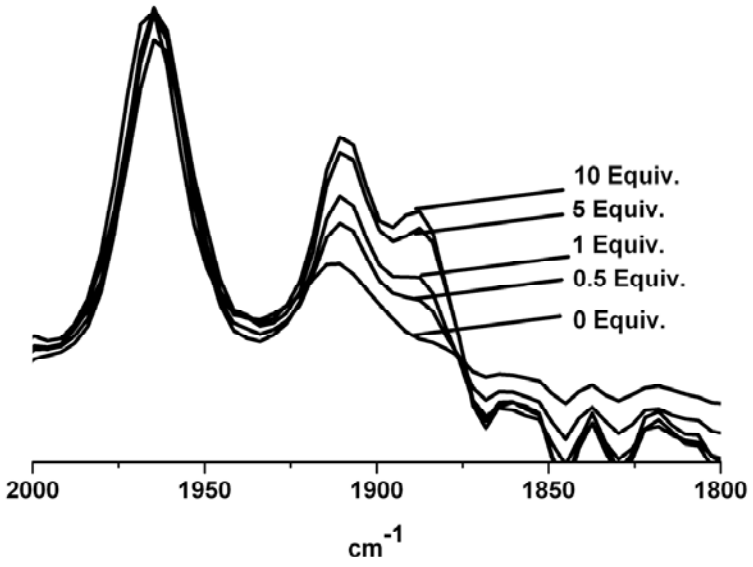

Figure S12. *In situ* ReactIR spectra of [**2**H]BAr^F_4 (CD_2Cl_2 solution) showing terminal hydride tautomer at -40 °C (1965, 1910 cm^{-1}) titrated with increasing equivs of $[NBu_4]BF_4$. The growth of the ammonium tautomer (1965, 1910 cm^{-1}) upon addition of BF_4^- is consistent with similar pK_a's of the ammonium and the terminal hydride tautomers. The spectra are normalized with respect to the band near 1970 cm^{-1}.

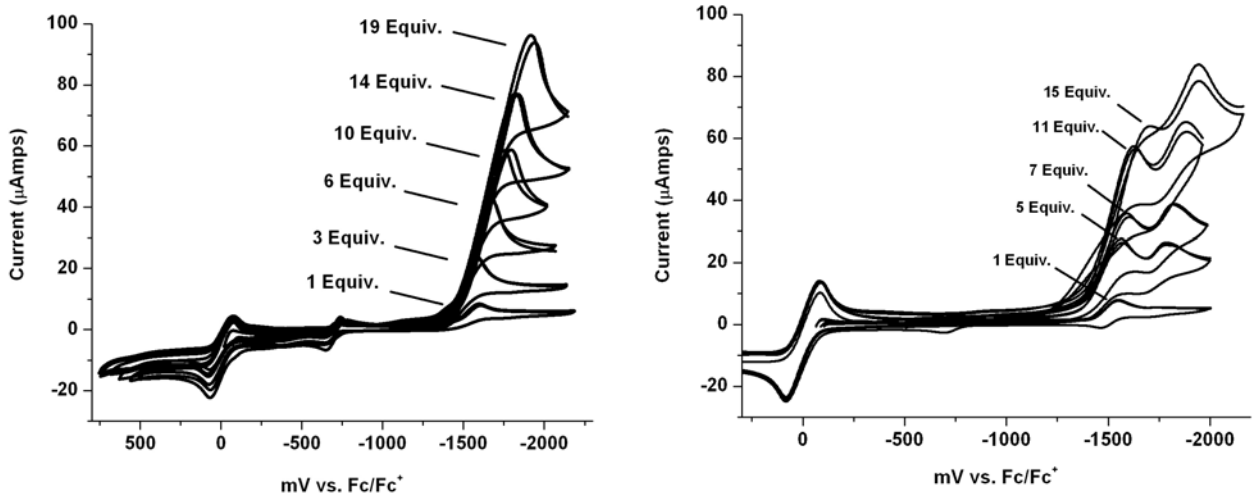

Figure S13. Cyclic voltammagrams for [**2**(*t*-H)]BF_4) (left) and [**3**(*t*-H)]BF_4 (right) (-20 °C, 1 mM catalyst, ~1 mM ferrocene) with increasing amounts of [$HPMe_2Ph$]BF_4 and $HBF_4{\cdot}Et_2O$, respectively. The presence of unprotonated **2** and **3** is seen at ~-200 mV. The event at ~-2 V for [**3**(*t*-H)]BF_4 is attributed to catalysis by [**3**(μ-H)]BF_4.

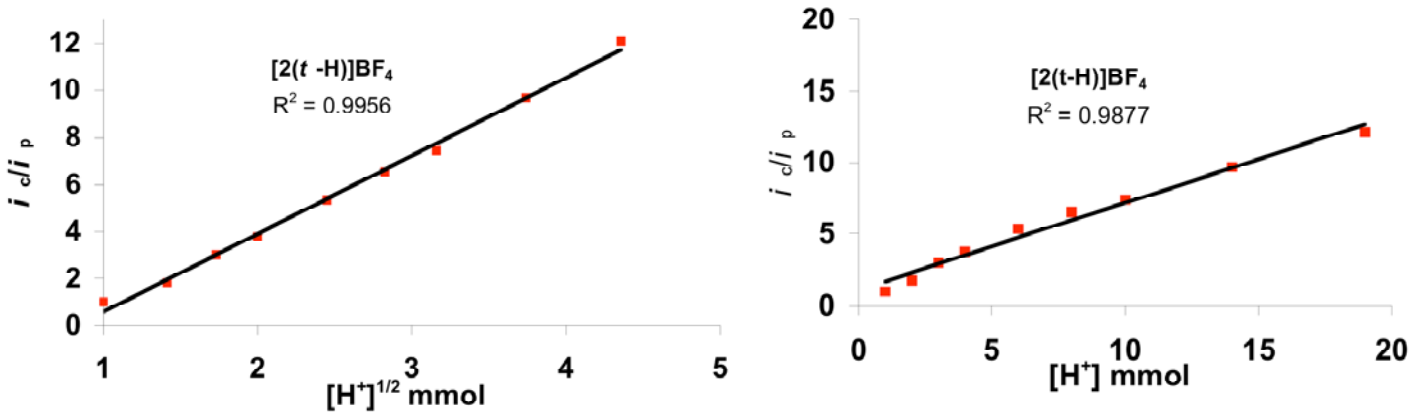

Figure S14. Plot of $[H^+]^{1/2}$ (left) and $[H^+]$ (right) vs. current (i_c/i_p) for [**2**(*t*-H)]BF_4 (-20 °C, 1 mM catalyst, $[HPMe_2Ph]BF_4$). i_c is the peak catalytic current, i_p is the peak current in the absence of acid.

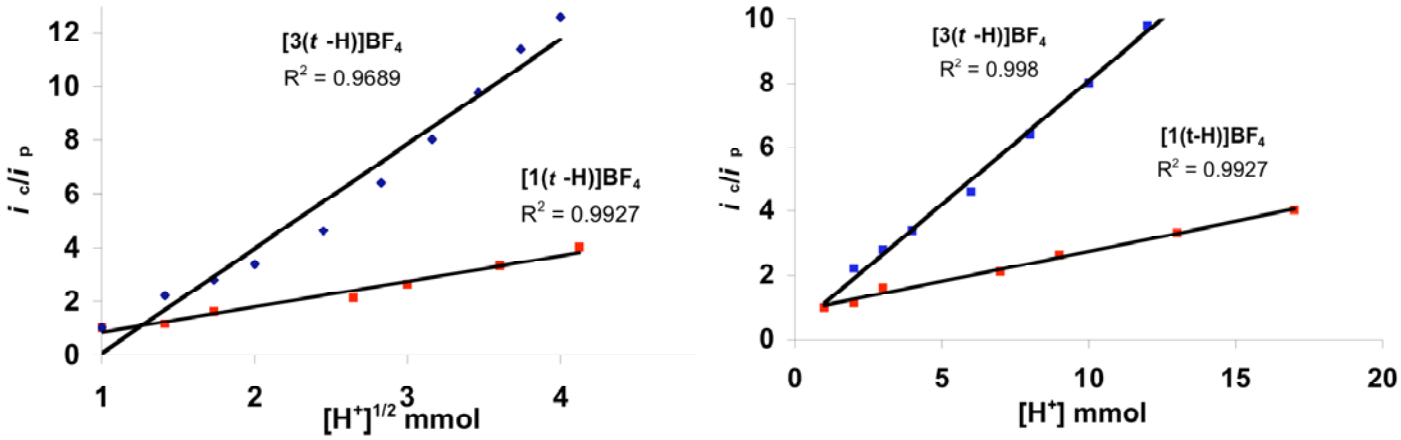

Figure S15. Plots of $[H^+]^{1/2}$ (left) and $[H^+]$ (right) vs. current (i_c/i_p) for [**1**(t-H)]BF_4 and [**3**(*t*-H)]BF_4 (-20 °C, 1 mM catalyst, $HBF_4{\cdot}Et_2O$).

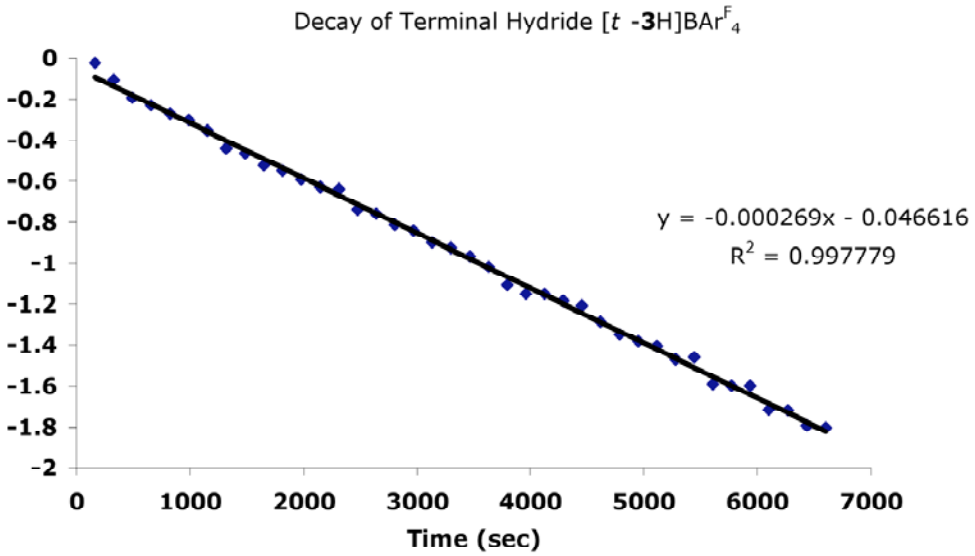

Figure S16. Plot of decay of terminal hydride [**3**(*t*-H)]BAr^F_4 (-10 °C, CH_2Cl_2, soln.) as assayed by ^1H NMR spectra. The products are isomers of [**3**(μ-H)]BAr^F_4. Scale on left shows ln(signal intensity) in arbitrary units.

3) Supporting References

1. Barton, B. E.; Rauchfuss, T. B. *Inorg. Chem.* **2008**, *47*, 2261-2263.
2. Song, L.-C.; Yang, Z.-Y; Bian, H.-Z.; Hu, Q.-M. *Organometallics*. **2004**, *23*, 3082-3084.
3. Yakelis, N. A.; Bergman, R. G. *Organometallics*. **2005**, 3579-3581.